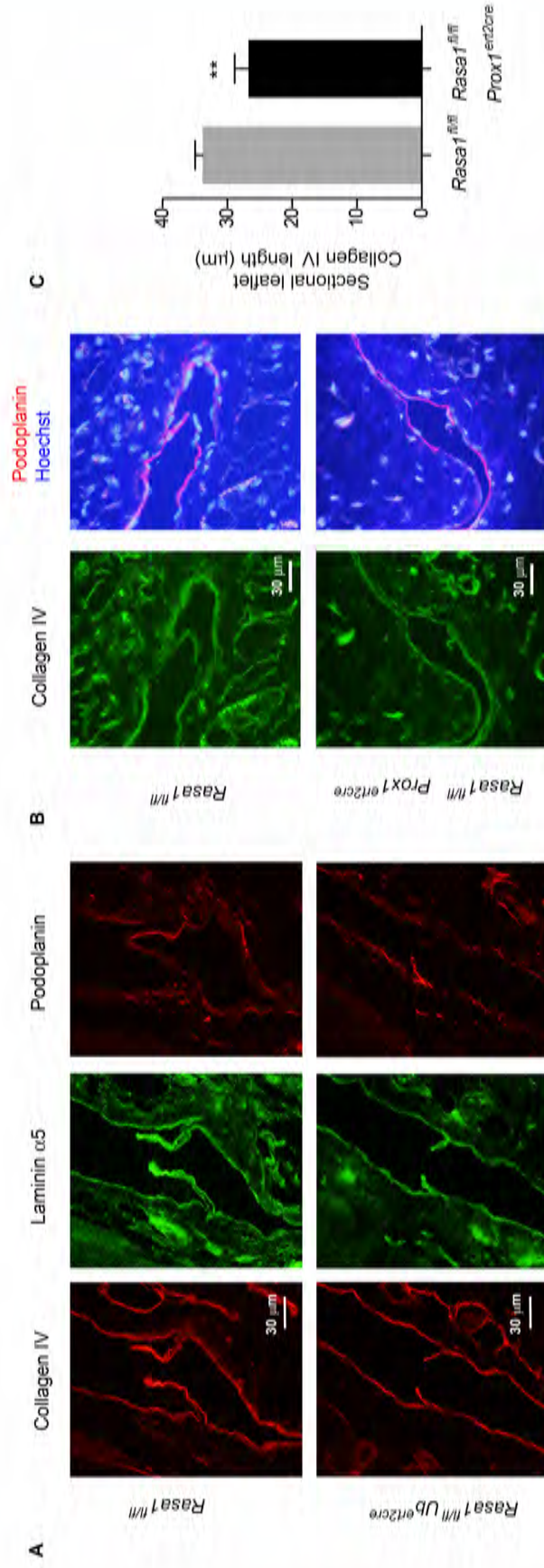
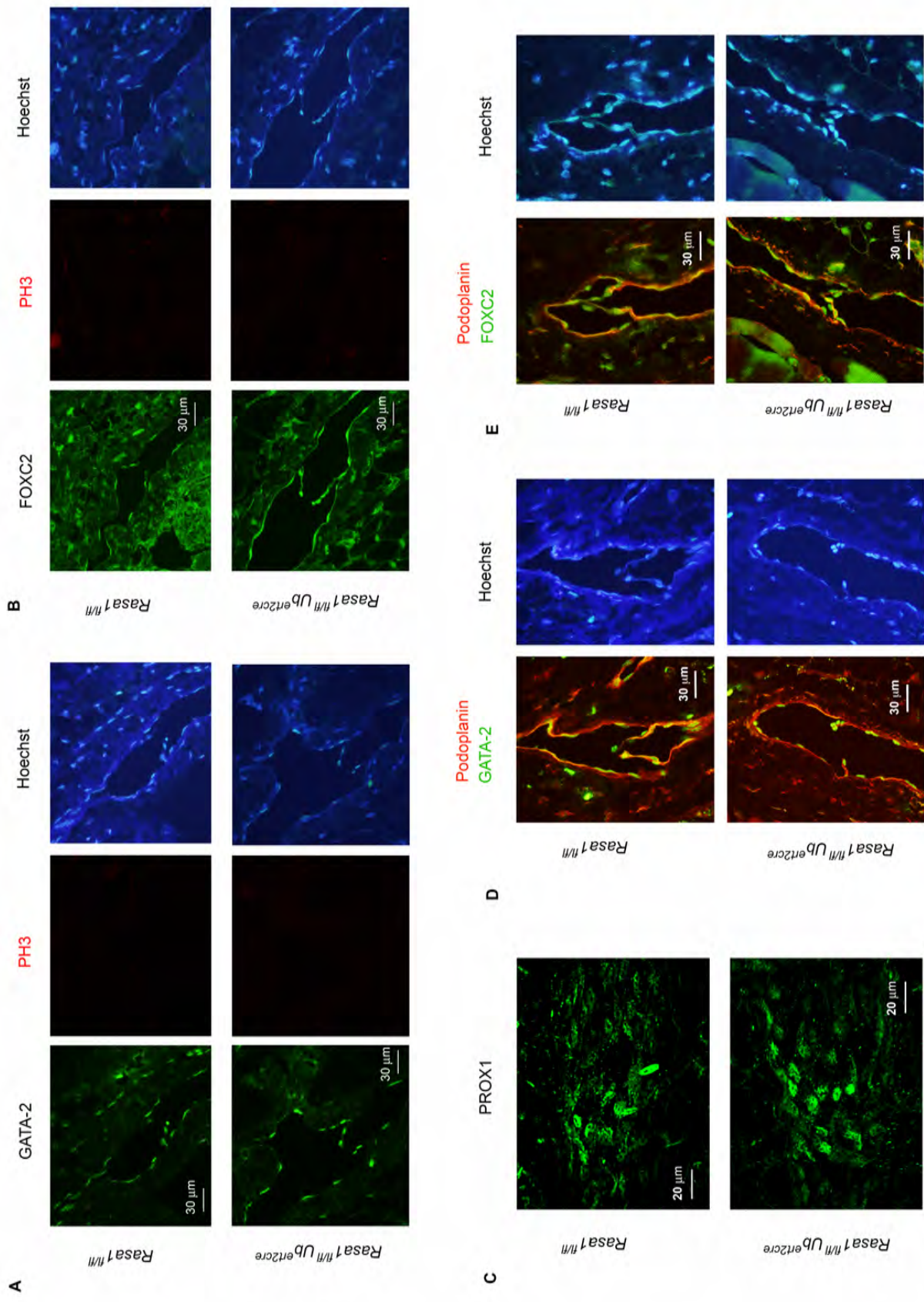


Supplemental Figure 1. Contractile activity of collecting LVs is not affected by induced loss of RASA1.

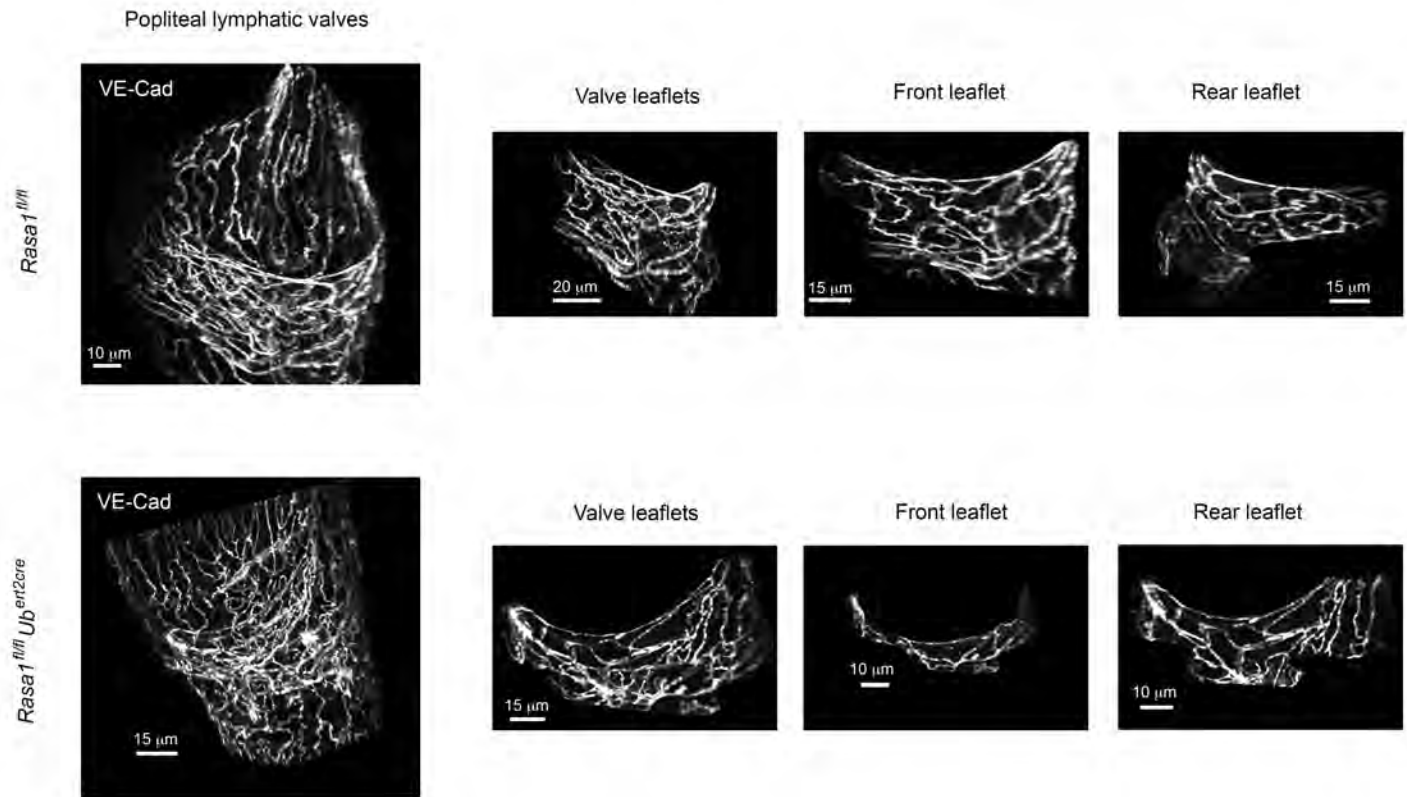
(A) Schematic representation of lymphatic contraction tests. Afferent popliteal LVs were trimmed to contain two valves (V1 and V2) and were cannulated at both ends with pipettes used to manipulate intraluminal pressure upstream (Pin) of V1 and downstream (Pout) of V2. An arrow indicates the direction of fluid flow as a result of vessel contraction. Vessel contraction amplitude and frequency at different Pin and Pout, which were changed in parallel, was determined by measurement of vessel diameter over time. The position of the diameter tracking window is shown. (B) Example traces from contraction tests performed with LVs from littermate *Rasa1^{fl/fl}* and *Rasa1^{fl/fl} Ub^{ert2cre}* mice administered tamoxifen-treated 9 weeks previously. Vessel diameter at different Pout and Pin over time is shown. (C) Summary plots of contraction tests performed with different vessels from littermate *Rasa1^{fl/fl}* (n=7) and *Rasa1^{fl/fl} Ub^{ert2cre}* mice (n=8). Shown is mean +/- SEM of contraction amplitude, frequency, ejection fraction and fractional pump flow, calculated as described in Methods.



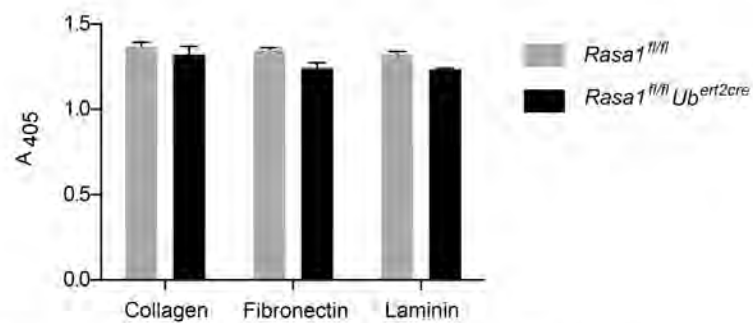
Supplemental Figure 2. Reduced ECM in LV valve leaflets of induced RASA1-deficient mice. (A) Sections of valves prepared from popliteal LVs from littermate *RasA1^{fl/fl}* and *RasA1^{fl/fl} Ub^{ert2cre}* mice administered tamoxifen 10 weeks previously were stained with antibodies against collagen IV and laminin alpha5. Shown are single color images adjacent to images of anti-podoplanin staining of serial sections to confirm lymphatic identity. (B) Sections of valves prepared from popliteal LVs from littermate *RasA1^{fl/fl}* and *RasA1^{fl/fl} Prox1^{ert2cre}* mice administered tamoxifen 8 weeks previously were stained with antibodies against collagen IV and podoplanin and with Hoechst dye to highlight nuclei. Shown are images of collagen IV staining and merged images of podoplanin and Hoechst staining. (C) Leaflet length based upon collagen IV images was measured for different valve leaflets from mice in (B). Shown is the mean + SEM leaflet length (*RasA1^{fl/fl}*, n=100; *RasA1^{fl/fl} Prox1^{ert2cre}*, n=50). **, p<0.001.



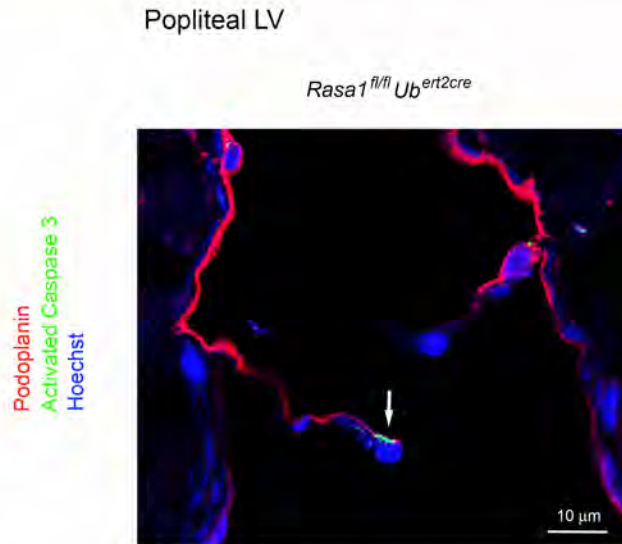
Supplemental Figure 3. Normal levels of expression of GATA2, FOXC2 and PROX1 transcription factors in LEC of LV valve leaflets of induced RASA1-deficient mice. *Rasa1^{fl/fl}* and *Rasa1^{fl/fl} Ubert2^{cre}* mice administered tamoxifen 1 week (A-C) or 10 weeks (D and E) previously. (A, B, D, E) Sections of popliteal LV valves were stained with antibodies against GATA2 (A and B), FOXC2 (B and E) and antibodies against PH3 to detect proliferating cells (A and B), podoplanin to confirm lymphatic identity (D and E) and Hoechst staining to indicate nuclei (A, B, D and E). (C) Whole mount preparations of popliteal LV were stained with an antibody against PROX1. Shown are confocal images of LV valves. For all panels, images are representative of at least 10 valves examined.



Supplemental Figure 4. Expression level and distribution of VE-Cadherin upon LEC in valve leaflets of LVs is not altered upon loss of RASA1. Popliteal LVs from *Rasa1^{fl/fl}* and *Rasa1^{fl/fl} Ub^{ert2cre}* mice treated with tamoxifen 10 weeks previously were stained with anti-VE-Cadherin antibodies and examined by confocal microscopy. Shown are images of entire valve regions, both leaflets and individual leaflets.



Supplemental Figure 5. RASA1-deficient LEC show normal adhesion to ECM proteins in vitro. Lung LEC were isolated from *Rasa1^{fl/fl}* and *Rasa1^{fl/fl} Ub^{ert2cre}* mice treated with tamoxifen 1 week previously and were cultured on plates coated with the indicated ECM proteins in the presence of PMA. After overnight culture, wells were washed and adherent cells were quantified using a colorimetric assay (absorbance at 405 nm). Shown is the mean + SEM of duplicate determinations for each ECM protein and LEC type.



Supplemental Figure 6. Anti-activated caspase 3 staining of LEC in LV leaflets of induced RASA1-deficient mice. Sections of popliteal LV valves from *Rasa1^{fl/fl}* and *Rasa1^{fl/fl} Ub^{ert2cre}* mice treated with tamoxifen 1 week previously were stained with antibodies against activated caspase 3 and podoplanin to identify apoptotic LEC and Hoechst to identify nuclei. Shown is an image of a valve from a *Rasa1^{fl/fl} Ub^{ert2cre}* mouse. Note the valve leaflet LEC with cytoplasmic activated caspase 3 indicative of early apoptosis (arrow). No apoptotic LEC were observed in leaflets of greater than 50 examined valves from *Rasa1^{fl/fl}* mice or greater than 40 examined other valves from *Rasa1^{fl/fl} Ub^{ert2cre}* mice.

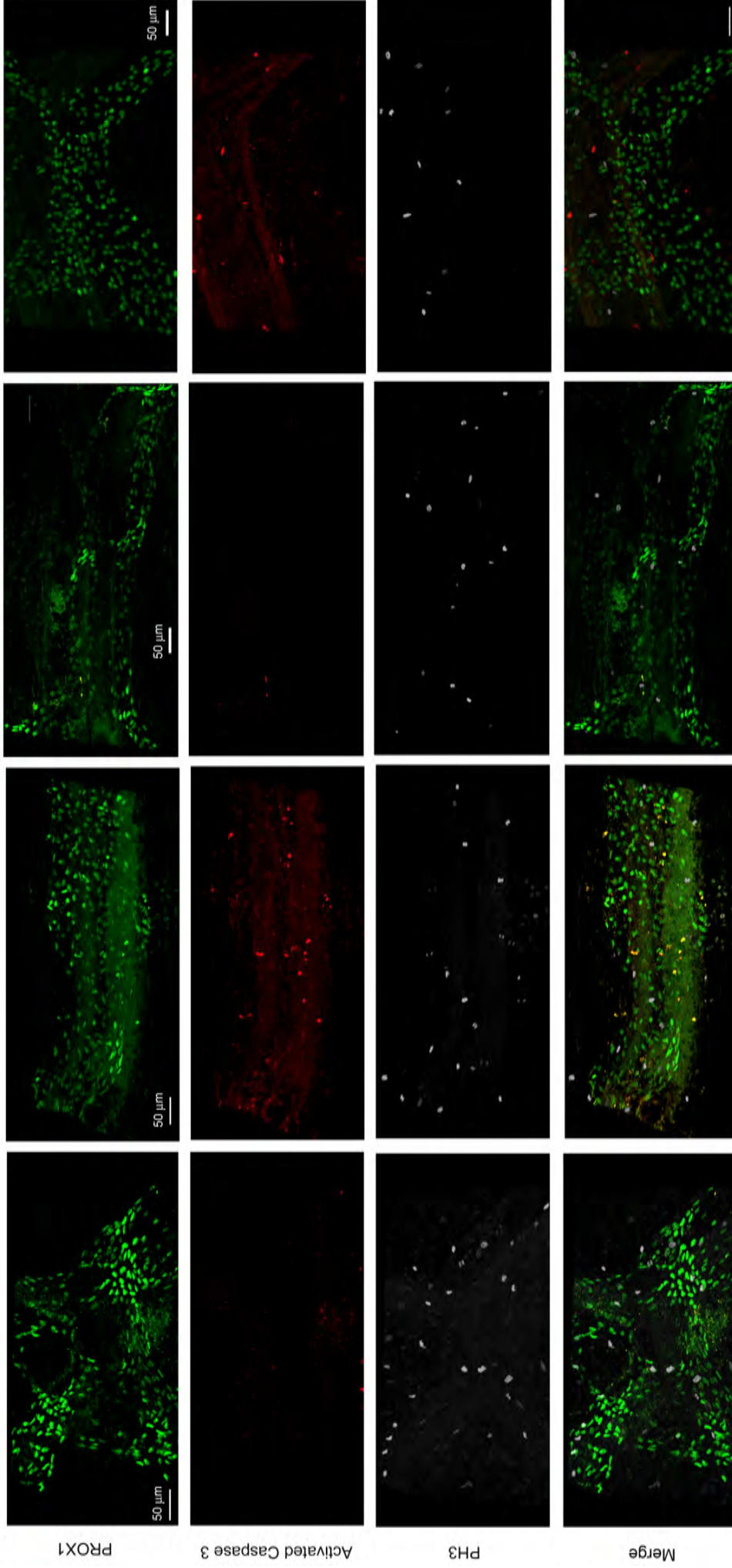
E15.5 TM - E17.5 analysis

Rasa1^{fl/fl}

Rasa1^{fl/fl} Ub^{ert2cre}

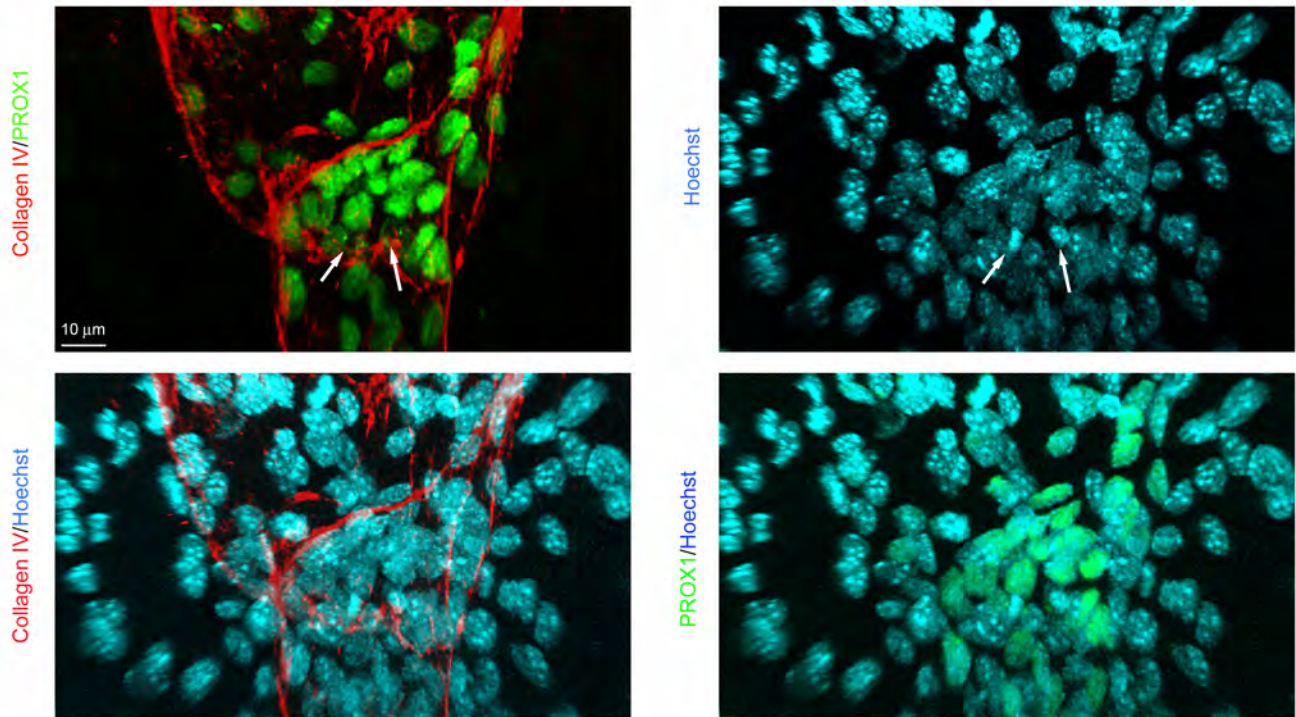
Rasa1^{fl/fl}

Rasa1^{fl/fl} Ub^{ert2cre}

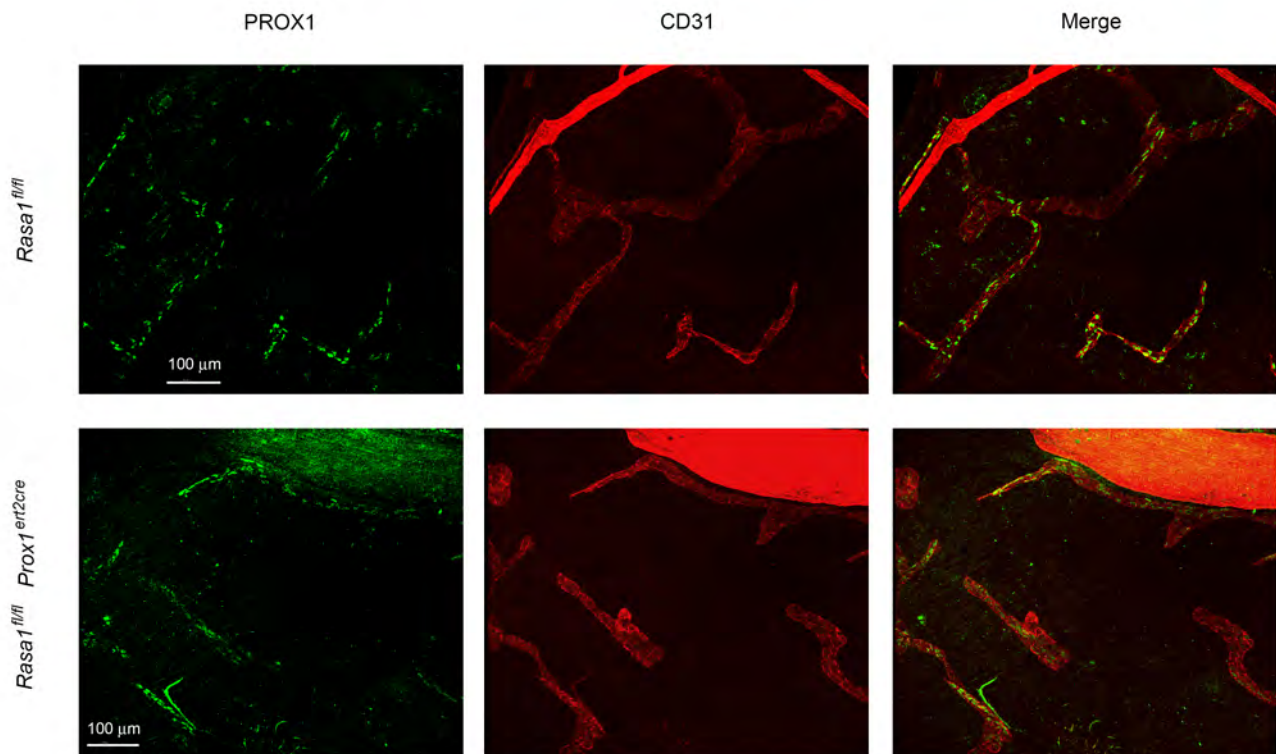


Supplemental Figure 7. Apoptosis of PROX1^{hi} LEC in developing LV valves of induced RASA1-deficient embryos. *Rasa1^{fl/fl}* and *Rasa1^{fl/fl} Ub^{ert2cre}* embryos were administered tamoxifen at E17.5 and E19.5 and stained with antibodies against PROX1, activated caspase 3 and PH3. Shown are confocal microscopic images of individual and merged antibody stains of representative mesenteric LV valve regions from the two types of mice at the different time points. Note the presence of PROX1^{hi} LEC in mesenteric LV of E17.5 *Rasa1^{fl/fl} Ub^{ert2cre}* embryos, some of which are stained with the anti-activated caspase 3 antibody and are in the process of apoptosis. Note also that absence of PROX1^{hi} LEC in LV of E19.5 *Rasa1^{fl/fl} Ub^{ert2cre}* embryos and lack of LEC apoptosis.

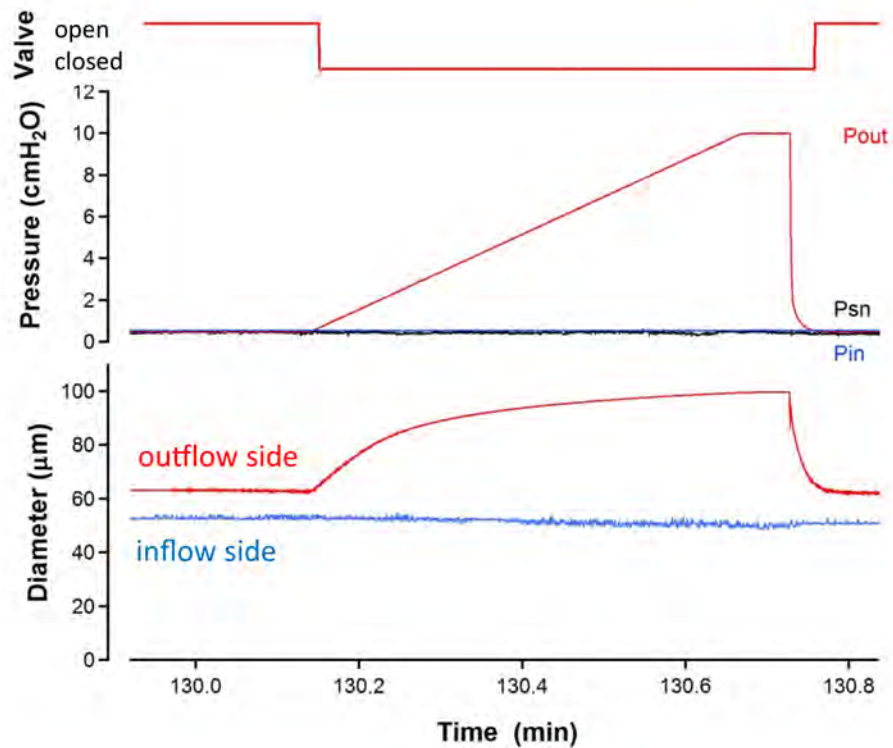
Rasa1^{fl/fl}Ub^{ert2cre}



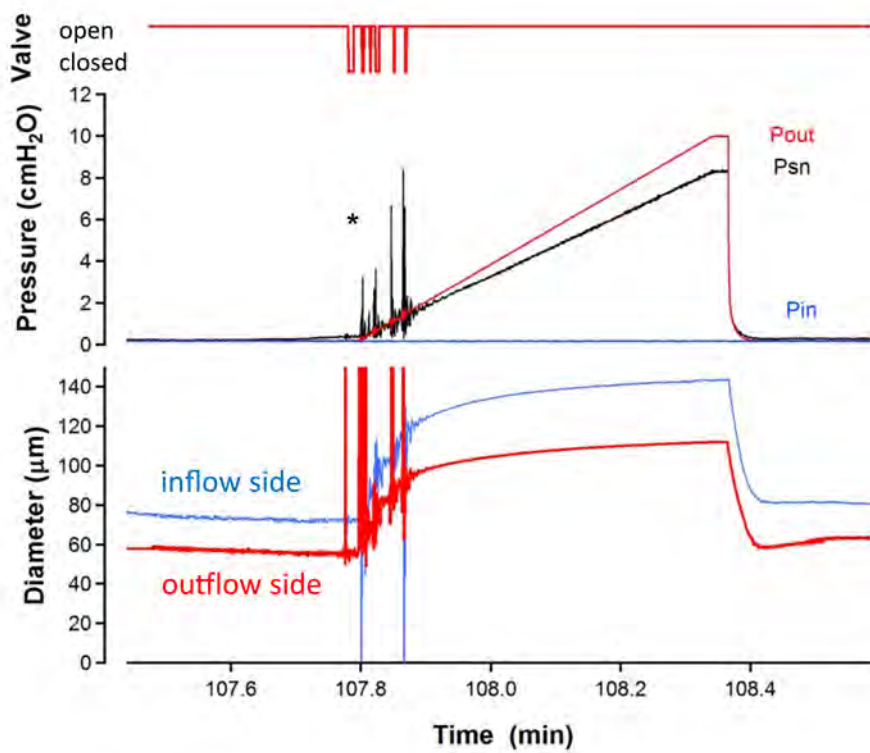
Supplemental Figure 8. Discontinuous ECM in developing LV valve leaflets of induced RASA1-deficient embryos. Confocal images are of the same LV valve from E17.5 *Rasa1^{fl/fl}Ub^{ert2cre}* embryos in Figure 10. Vessels were also stained with Hoechst to highlight nuclei. Note the presence of two leaflet LEC (arrows) with peripheral PROX1 staining and condensed nuclei indicative of apoptosis.



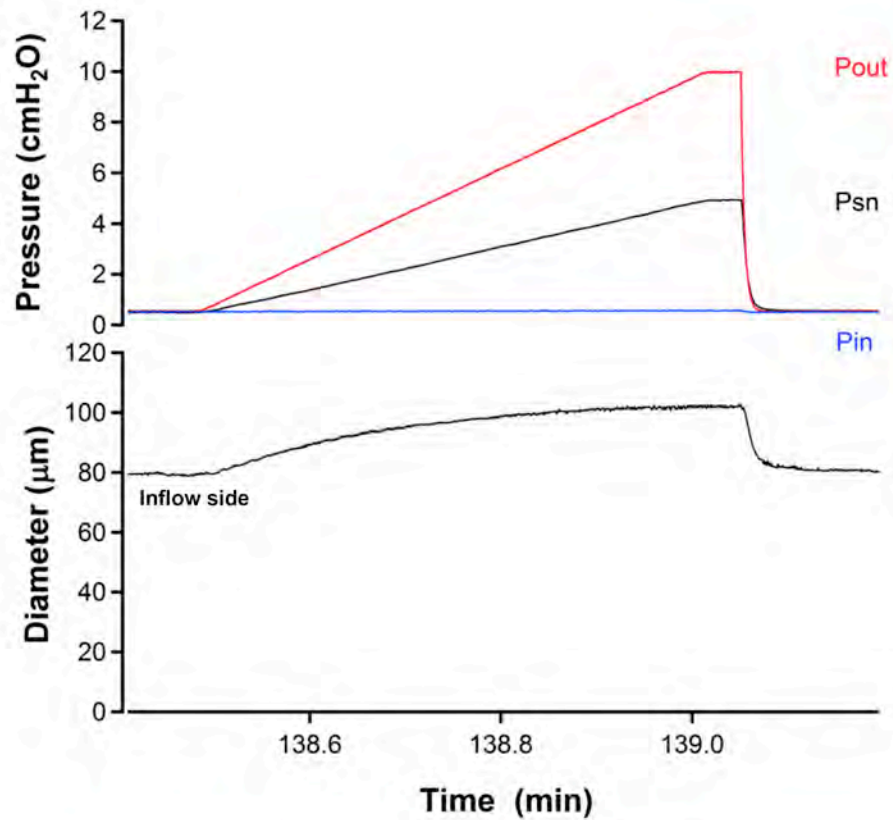
Supplemental Figure 9. LV valve dysfunction in adult induced RASA1-deficient mice precedes LV hyperplasia. Diaphragms from *Rasa1^{fl/fl} Prox1^{ert2cre}* mice with defective mesenteric LV valves shown in Figure 4 (represented by orange diamonds and green triangles) and diaphragms from littermate control *Rasa1^{fl/fl}* mice (all with normal mesenteric LV valves) were stained with antibodies against PROX1 and CD31 to identify LEC. Shown are representative areas of diaphragms. Note the absence of LV hyperplasia in the *Rasa1^{fl/fl} Prox1^{ert2cre}* diaphragms.



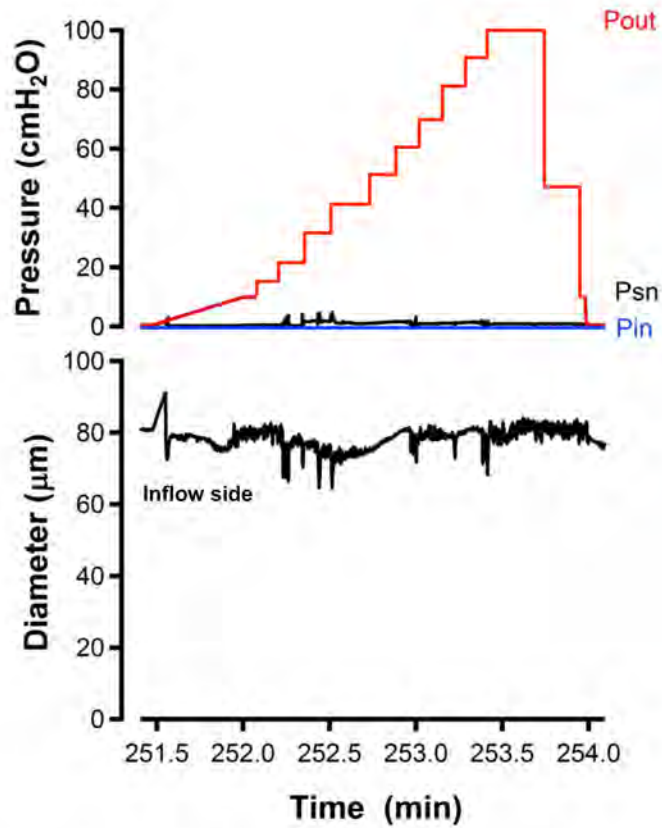
Supplemental Video 1. Example low pressure back-leak test of a popliteal LV valve from a control *Rasa1^{fl/fl}* mouse treated with tamoxifen 1 week earlier showing normal valve closure. Valve position (top trace) was determined by placing a video densitometry window at the base of the valve and then using a thresh-holding algorithm to convert the analog signal to binary (open/closed). Valve closure prevents diameter on the inflow side from increasing during the Pout ramp.



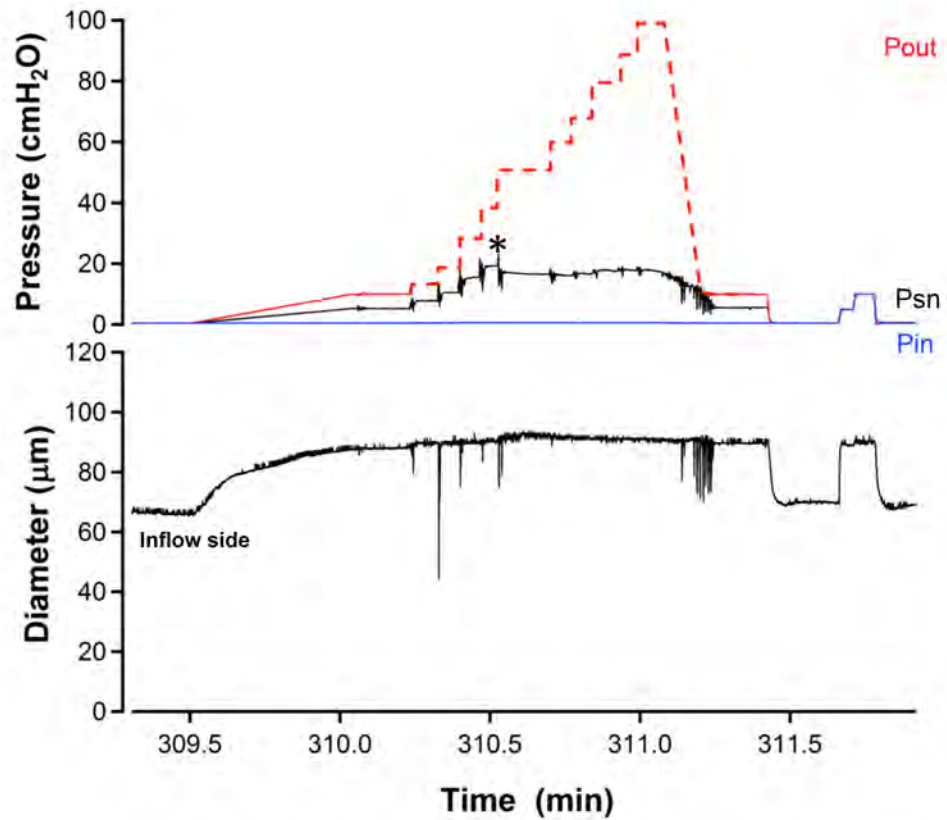
Supplemental Video 2. Example low pressure back-leak test of a leaky popliteal LV valve from a *Rasa1^{fl/fl} Ub^{ert2cre}* mouse treated with tamoxifen 1 week earlier showing failed valve closure. At asterisk the outflow line was tapped to generate rapid pressure spikes and encourage valve closure, but the valve failed to close completely or stay closed.



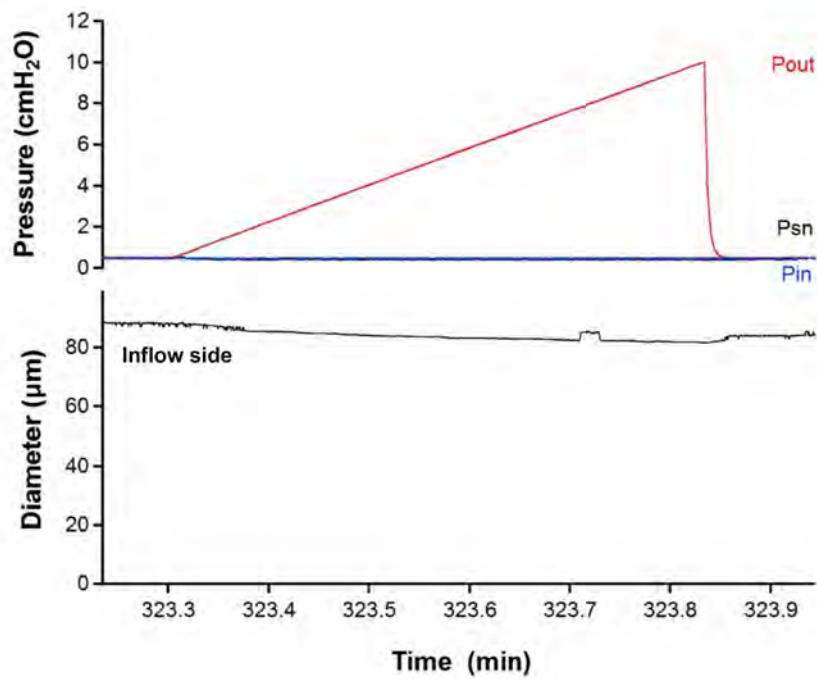
Supplemental Video 3. Low pressure back-leak test of a popliteal LV valve from a *Rasa1^{fl/fl} Prox1^{ert2cre}* mouse treated with tamoxifen 11 weeks earlier showing failed valve closure. The valve is represented by grey circles in Figure 4A-C.



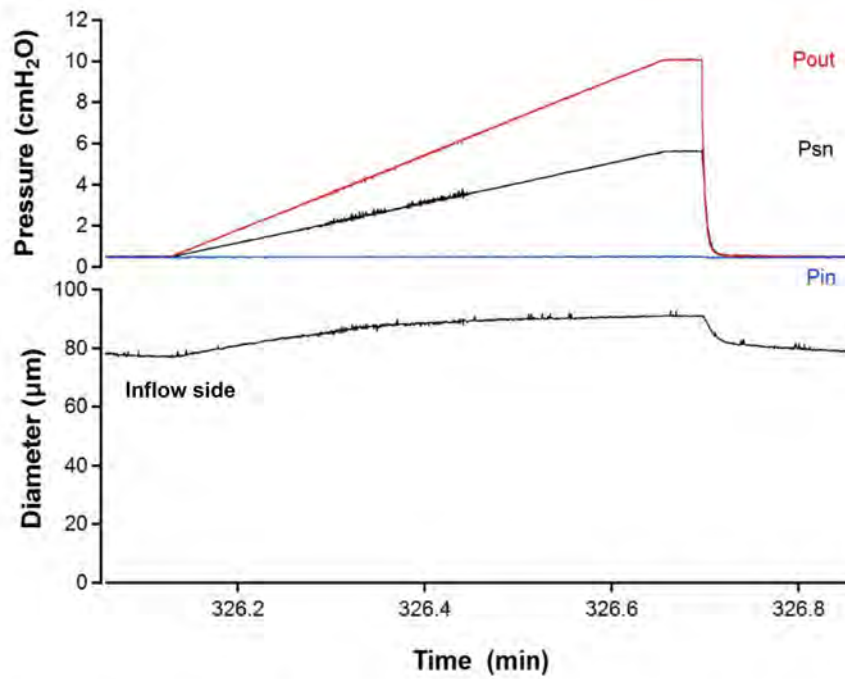
Supplemental Video 4. Example high pressure back-leak test of a popliteal LV valve from a control *Rasa1^{fl/fl}* mouse treated with tamoxifen 9 weeks earlier showing normal valve closure. Same recording shown in Figure 3B.



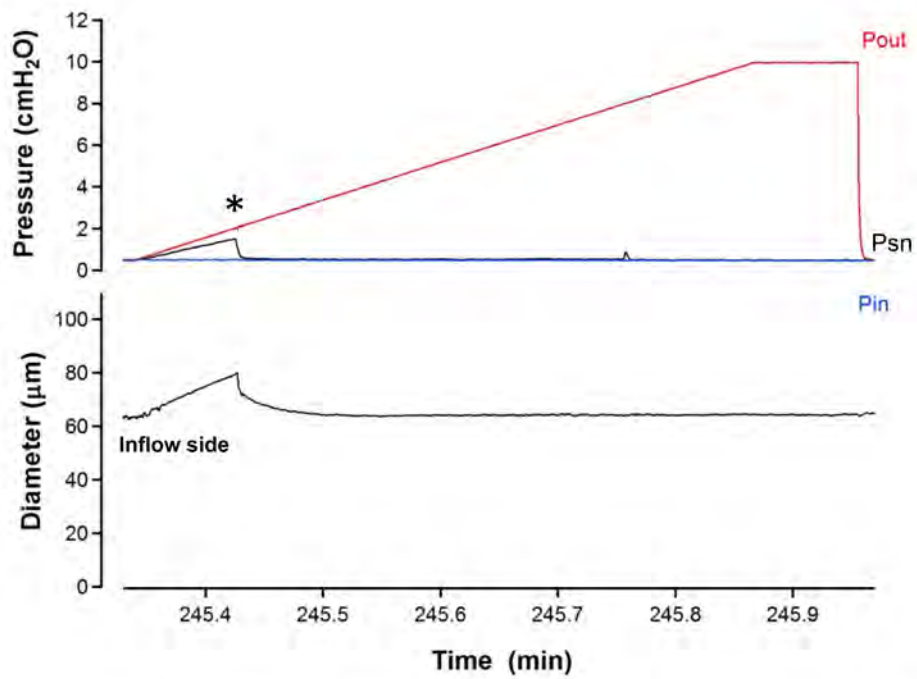
Supplemental Video 5. High pressure back-leak test of a popliteal LV valve from a *Rasa1^{fl/fl} Prox1^{ert2cre}* mouse treated with tamoxifen 11 weeks earlier showing valve closure at a Pout of 50 cm H₂O. The valve is represented by red triangles in Figure 4A-C. Asterisk indicates the time at which valve closure occurred after which Psn failed to rise in proportion to Pout.



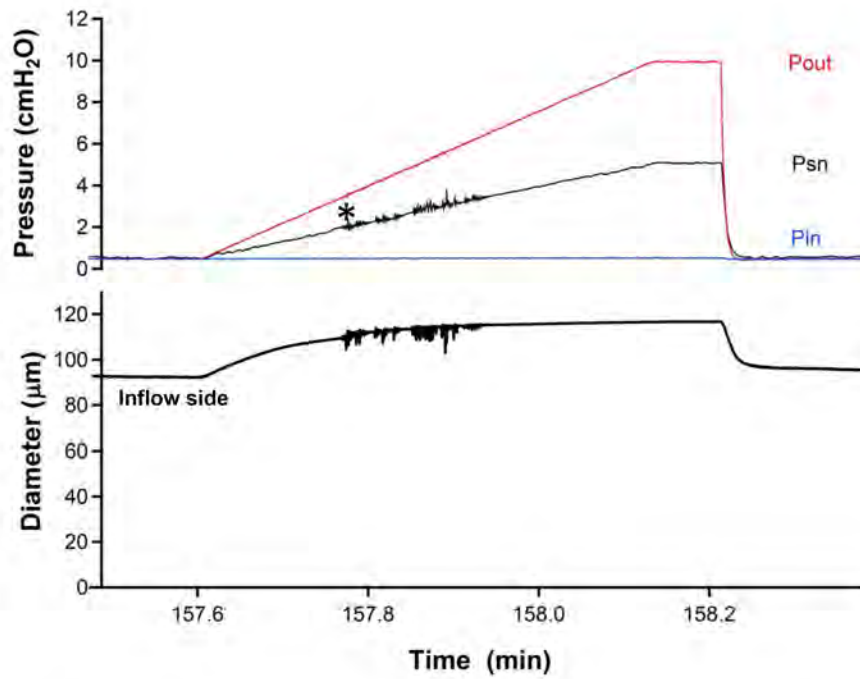
Supplemental Video 6. Example low pressure back-leak test of a mesenteric LV valve from a *Rasa1^{fl/fl}* mouse treated with tamoxifen 20 weeks earlier showing normal valve closure.



Supplemental Video 7. Low pressure back-leak test of a mesenteric LV valve from a *Rasa1^{fl/fl} Prox1^{ert2cre}* mouse treated with tamoxifen 20 weeks earlier showing failed valve closure. The valve is represented by blue circles in Figure 4D-F.



Supplemental Video 8. Example low pressure back-leak test of a popliteal LV valve from a *Rasa1^{fl/R780Q} U^{B^{ert2cre}}* mouse treated with tamoxifen 12 weeks earlier showing normal valve closure. Asterisk indicates the time at which spontaneous valve closure occurred as Pout increased.



Supplemental Video 9. Example low pressure back-leak test of a popliteal LV valve from a *Rasa1^{fl/R780Q} U^bert2^{cre}* mouse treated with tamoxifen 23 weeks earlier showing failed valve closure. At asterisk the outflow line was tapped to generate rapid pressure spikes and encourage valve closure, but the valve failed to close completely.

Supplemental Methods

Tamoxifen administration. Mice were given 2 i.p. injections of tamoxifen (0.05 mg/g body weight per injection, dissolved in corn oil; Sigma) on consecutive days. For most studies, tamoxifen was administered at 2 months of age and mice were euthanized at different times after tamoxifen as indicated. For survival studies, mice were administered tamoxifen at 3 weeks of age and either died from chylothorax or were euthanized if they showed signs of labored breathing, which is indicative of this condition. For lymphatic valve development studies, tamoxifen was administered to pregnant dams at 13.5 or 15.5 days after detection of vaginal plugs (1 i.p. injection of tamoxifen as above) and embryos were harvested at E17.5, E18.5 or E19.5.

Vessel contraction and pumping tests. Mice were anesthetized with sodium pentobarbital (60 mg/kg, i.p.) and placed on a heating pad. The skin over the lower leg was shaved and an incision made to expose the underlying popliteal collecting lymphatic vessels running in parallel to the saphenous vein. A popliteal lymphatic vessel (1-2 mm in length) was removed and pinned with 40- μ m stainless steel wire to a Sylgard dish. The mouse was then euthanized with an injection of KCl (0.2 M, i.c.). After removal of fat and connective tissue a 2-valve vessel segment was cannulated onto two micropipettes (40 and 60 μ m tip, o.d., for the inflow and outflow ends of the vessel, respectively) in a 3 ml chamber and transferred to the stage of an inverted microscope, where it was heated to 37°C and superfused with Krebs buffer (0.5 ml/min) for at least 30 min until a consistent pattern of spontaneous contractions developed. Krebs buffer contained (in mM): NaCl, 146.9; KCl, 4.7; CaCl₂·2H₂O, 2; MgSO₄, 1.2; NaH₂PO₄·H₂O, 1.2; NaHCO₃, 3; sodium-

Hepes, 1.5; D-glucose, 5 (pH 7.4 at 37⁰C). The cannulation pipettes contained Krebs buffer plus 0.5% purified BSA (pH 7.4 at 37⁰C). All chemicals were obtained from Sigma, with the exception of BSA (US Biochemicals), MgSO₄ and sodium-Hepes (Fisher Scientific).

Contraction tests assessed the strength of spontaneous lymphatic contractions at different pressures spanning the physiological range presumably experienced by popliteal lymphatics in vivo. Pin and Pout were lowered in unison (i.e. no net gradient for flow) to 2, 1, and 0.5 cm H₂O and then raised to 3, 5, 8, and 10 cm H₂O while diameter was measured continuously as shown in Figure 1. Pressure control and pressure / diameter measurements were recorded digitally as described previously (1). At each pressure level the vessel was maintained for at least 2 min or until a sufficient number of spontaneous contractions occurred to obtain a reliable measurement of contraction amplitude and frequency. Contraction amplitude at each pressure was calculated as the difference between end-diastolic diameter (EDD) and end-systolic diameter (ESD). Amplitude was normalized to the passive diameter of the vessel recorded at the respective pressure in Ca²⁺-free Krebs (plus 3 mM EDTA) after the contraction and pumping tests were completed (2). Contraction frequency (FREQ) was calculated from the number of contractions per minute. Ejection fraction (EF) = $(EDD^2 - ESD^2)/EDD^2$, as appropriate for a cylindrical vessel. Fractional pump flow = FREQ x EF.

Pumping tests assessed the ability of a spontaneously contracting vessel to pump against an adverse pressure gradient (1). Pin was held at 0.5 cm H₂O while Pout was raised ramp-

wise from 0.5 to ~10 cm H₂O and diameter was measured upstream from the outflow valve. Once P_{out} exceeded P_{in}, a normal output valve would typically remain closed in diastole and opened transiently in systole as the vessel contracted and generated an intraluminal pressure pulse. A closed outflow valve prevented the rising level of P_{out} from being transmitted upstream and distending the vessel in diastole, so that the typical response of a normal vessel was a modest myogenic constriction in response to P_{out} elevation (Figure 1) (3). Eventually P_{out} reached a level beyond which the vessel could no longer open the output valve in systole: that value of P_{out} was referred to as the pump limit (P_{limit}).

Valve closure tests. To assess the adverse pressure gradient required for valve closure, the vessel segment was shortened to one valve and superfused with Ca²⁺-free Krebs to prevent spontaneous contractions (Figure 3). A servo-nulling micropipette with tip diameter ~3 μm was inserted through the vessel wall upstream on the upstream side of the valve to measure the local pressure change (P_{sn}) at that site (4). P_{in} and P_{out} were raised simultaneously from 0.5 to 10 cm H₂O in order to confirm/adjust the calibration of the servo-nulling system. P_{in} was held at 0.5 cm H₂O while P_{out} was raised ramp-wise (4 cm H₂O/min) from 0.5 to ~35 cmH₂O or until the valve closed. The valve was biased to be open initially at P_{in}=P_{out} and normal valves closed when P_{out} exceeded P_{in} by only a small degree. The pressure ramp was repeated 3 times, with P_{out} returned to the baseline pressure each time. P_{in} and P_{out} were then lowered to 0.3, 0.2 and 0.1 cm H₂O and the test repeated, and then raised to 1, 2, 3, 5, 8 and 10 cm H₂O, again repeating the test at each baseline pressure. Closure of the valve during the P_{out} ramp produced a sharp fall in

P_{sn} and the difference in pressures ($P_{out}-P_{in}$) at that point in time was noted. For subsequent data analysis, the pressure difference associated with valve closure at each baseline pressure was plotted as a function of the normalized diameter of the vessel on the upstream side (D/D_{max}). The data have not been corrected to take into account the resistances of the cannulating pipettes and thus the actual values of ($P_{out}-P_{in}$) are overestimated; however the cannulating pipettes were cleaned and reused after each experiment and the same pipettes were used for all experimental groups.

Valve back-leak assays. To assess the ability of a closed valve to prevent pressure back leak, the same configuration described for the closure test was used. For low-pressure back leak tests, P_{in} was set to 0.5 cm H₂O and P_{out} was elevated ramp-wise from 0.5 to 10 cm H₂O while the servo-nulling pipette detected any rise in pressure upstream from the valve. Normal valves closed spontaneously as P_{out} exceeded P_{in} (usually by less than 1 cm H₂O), but if the valve did not close on its own, the output line was tapped gently to produce pressure spikes and facilitate closure (Figure 4A, right panel shows an example). The P_{out} ramp was repeated 3 times. After the experiment, the P_{sn} data, recorded at 30 Hz, were binned in 1 cm H₂O intervals for plotting and statistical tests. High pressure back leak tests were conducted in the same manner, except that P_{in} was held at 0.5 cm H₂O while P_{out} was stepped from 10 to 100 cm H₂O in increments of 10 cm H₂O using an adjustable reservoir, to prevent pressures higher than 50 cm H₂O from damaging the pressure transducers.

Whole mount immunofluorescence staining. Popliteal lymphatic vessels were fixed in situ in 1% paraformaldehyde in PBS overnight before dissection from surrounding connective tissue. Diaphragms from adult mice and mesenteries from embryos were fixed in 4% paraformaldehyde in PBS for 1 hour. Tissues were blocked by incubation in PBS/0.3% Triton-X100/10% donkey serum for 4 hours followed by overnight incubation with the following primary antibodies in PBS/0.3% Triton-X100: rabbit anti-PROX1 (ab101851, Abcam), goat anti-PROX1 (AF2727, R&D Systems), rat anti-CD31 (MEC13.3, BD Biosciences), goat anti-alpha-9 integrin (AF3827, R&D Systems), goat anti-VE-Cadherin (AF1002, R&D Systems), rabbit anti-activated caspase 3 (AF835, R&D Systems), goat anti-collagen IV (1340-01, Southern Biotechnology), mouse anti-SMA-Alexa Fluor 488 (1A4, Novus), mouse anti-PH3-Alexa Fluor 488 and -Alexa Fluor 647 (3H10, Millipore). Secondary antibodies used were species-specific anti-immunoglobulin donkey F(ab)₂ fragments coupled to Alexa Fluor 488, 594 or 647 (705-546-147, 711-546-152, 712-586-150, 705-586-147, 705-606-147, 712-606-153, 711-606-152, Jackson ImmunoResearch) and were incubated with tissues in PBS/0.3% Triton-X100 for 2 hours before mounting and viewing on a Leica SP5 X confocal microscope (Leica Microsystems). Images were deconvolved and analyzed using AutoQuant X3 (Media Cybernetics) and Imaris (Bitplane) software respectively.

Tissue section immunofluorescence. Popliteal lymphatic vessels were fixed in situ in 3.75% formalin overnight and embedded in paraffin. Chest walls from mice that exhibited chylothorax were similarly fixed and decalcified before paraffin embedding. Five micrometer sections of tissues were dehydrated and antigen retrieval was performed

with a Diva de-cloaking kit (Biocare Medical). Sections were blocked for 1 hour using tyramide signal amplification (TSA) blocking buffer (Perkin Elmer) and incubated for 1 hour with the following primary antibodies in PBS: goat anti-FOXC2 (NB100-1269, Novus), goat anti-GATA2 (AF2046-SP, R&D Systems), goat anti-collagen IV, rabbit anti-laminin alpha-5 (NBP1-66514, Novus), rabbit anti-LYVE1 (ab14917, Abcam), rabbit anti-activated caspase 3, mouse anti-PH3 (3H10, Millipore), and hamster anti-podoplanin (8.1.1, provided by Y. Hong, University of Southern California, Los Angeles, California, USA). Secondary antibodies used were species-specific anti-immunoglobulin donkey F(ab)₂ fragments coupled to biotin Alexa Fluor 488 or 594 (715-546-151, 705-546-147, 711-546-152, 705-586-147, 715-586-151, 107-586-142, for detection of collagen IV, activated caspase 3, PH3, LYVE-1 and podoplanin) or biotin (711-065-152, 705-066-147, Jackson ImmunoResearch; for detection of all other antigenic targets) that were incubated with sections for 30 min in PBS. For TSA amplification, sections were incubated with streptavidin-HRP for 30 min in PBS before addition of TSA substrate for 10 minutes (Perkin Elmer). Sections were counterstained with Hoechst (Invitrogen) to identify nuclei. Mounted sections were viewed on a BX60 upright fluorescence microscope equipped with a digital camera (Nikon).

Flow cytometry. Pleural effusion cells from mice with chylothorax were stained with TCRβ-FITC (H57-597, BD Biosciences) and B220-APC-Cy7 antibodies (RA3-6B2, BD Biosciences). Cell staining was analyzed by flow cytometry on a FACSCanto (BD Biosciences).

Adhesion assays. Mouse lung LECs were isolated as described (5). 2×10^4 LECs in 200 μ l of DMEM, 20% FBS with 50ng/ml PMA (Sigma) were added to wells of a 96-well tissue culture plate pre-coated with laminin, fibronectin, or collagen (4ug/ml; Sigma). After overnight culture at 37°C, wells were washed three times with DMEM to remove non-adherent cells, and 200 μ l of substrate solution (6mg/ml Sigma 104 phosphatase substrate in 50mM Na Acetate buffer pH 5.0, 0.1% Triton X-100) was added to each well. The plate was incubated at 37°C for 1 h, and the reactions were stopped by addition of 50 μ l 3M NaOH. Absorbance at 405 nm was measured on a microplate reader.

References

1. Davis MJ, Scallan JP, Wolpers JH, Muthuchamy M, Gashev AA, and Zawieja DC. Intrinsic increase in lymphangion muscle contractility in response to elevated afterload. *Am J Physiol Heart Circ Physiol*. 2012;303(7):H795-808.
2. Scallan JP, and Davis MJ. Genetic removal of basal nitric oxide enhances contractile activity in isolated murine collecting lymphatic vessels. *J Physiol*. 2013;591(8):2139-56.
3. Scallan JP, Wolpers JH, and Davis MJ. Constriction of isolated collecting lymphatic vessels in response to acute increases in downstream pressure. *J Physiol*. 2013;591(2):443-59.
4. Sabine A, Bovay E, Demir CS, Kimura W, Jaquet M, Agalarov Y, Zangger N, Scallan JP, Graber W, Gulpinar E, et al. FOXC2 and fluid shear stress stabilize postnatal lymphatic vasculature. *J Clin Invest*. 2015;125(10):3861-77.
5. Lapinski PE, Kwon S, Lubeck BA, Wilkinson JE, Srinivasan RS, Sevick-Muraca E, and King PD. RASA1 maintains the lymphatic vasculature in a quiescent functional state in mice. *J Clin Invest*. 2012;122(2):733-47.